

# High-Resolution Ultraviolet Spectra of the Dwarf Seyfert 1 Galaxy NGC 4395: Evidence for Intrinsic Absorption<sup>1</sup>

D.M. Crenshaw<sup>2</sup>, S.B. Kraemer<sup>3</sup>, J.R. Gabel<sup>4</sup>, H.R. Schmitt<sup>5</sup>, A.V. Filippenko<sup>6</sup>, L.C. Ho<sup>7</sup>,  
J.C. Shields<sup>8</sup>, and T.J. Turner<sup>9</sup>

## ABSTRACT

We present ultraviolet spectra of the dwarf Seyfert 1 nucleus of NGC 4395, obtained with the *Far Ultraviolet Spectroscopic Explorer (FUSE)* and the *Hubble Space Telescope's* Space Telescope Imaging Spectrograph at velocity resolutions of 7 to 15 km s<sup>-1</sup>. We confirm our earlier claim of C IV absorption in low-resolution UV spectra and detect a number of other absorption lines with lower ionization potentials. In addition to the Galactic lines, we identify two kinematic components of absorption that are likely to be intrinsic to NGC 4395. We consider possible origins of the absorption, including the interstellar medium (ISM) of

---

<sup>1</sup>Based on observations made with the NASA/ESA *Hubble Space Telescope*, obtained at the Space Telescope Science Institute, which is operated by the Association of Universities for Research in Astronomy, Inc., under NASA contract NAS 5-26555; these observations are associated with proposal GO-9362. Also based on observations made with the NASA-CNES-CSA *Far Ultraviolet Spectroscopic Explorer*. *FUSE* is operated for NASA by Johns Hopkins University under NASA contract NAS5-32985.

<sup>2</sup>Department of Physics and Astronomy, Georgia State University, Astronomy Offices, One Park Place South SE, Suite 700, Atlanta, GA 30303; crenshaw@chara.gsu.edu.

<sup>3</sup>Catholic University of America and Laboratory for Astronomy and Solar Physics, NASA's Goddard Space Flight Center, Code 681, Greenbelt, MD 20771; stiskraemer@yancey.gsfc.nasa.gov.

<sup>4</sup>Center for Astrophysics and Space Astronomy, University of Colorado, 389 UCB, Boulder, CO 80309-0389; Jack.Gabel@colorado.edu.

<sup>5</sup>National Radio Astronomy Observatory, 520 Edgemont Road, Charlottesville, VA 22903; hschmitt@nrao.edu.

<sup>6</sup>Department of Astronomy, University of California, Berkeley, CA 94720-3411; alex@astro.berkeley.edu.

<sup>7</sup>The Observatories of the Carnegie Institution of Washington, 813 Santa Barbara Street, Pasadena, CA 91101-1292; lho@ociw.edu.

<sup>8</sup>Department of Physics and Astronomy, Ohio University, Athens, OH 45701-2979; shields@helios.phy.ohiou.edu.

<sup>9</sup>Joint Center for Astrophysics, University of Maryland, Baltimore County, 1000 Hilltop Circle, Baltimore, MD 21250; turner@lucretia.gsfc.nasa.gov.

NGC 4395, the narrow-line region (NLR), outflowing UV absorbers, and X-ray “warm absorbers.” Component 1, at a radial velocity of  $-770 \text{ km s}^{-1}$  with respect to the nucleus, is only identified in the C IV  $\lambda 1548.2$  line. It most likely represents an outflowing UV absorber, similar to those seen in a majority of Seyfert 1 galaxies, although additional observations are needed to confirm the reality of this feature. Component 2, at  $-114 \text{ km s}^{-1}$ , most likely arises in the ISM of NGC 4395; its ionic column densities cannot be matched by photoionization models with a power-law continuum. Our models of the highly ionized X-ray absorbers claimed for this active galactic nucleus indicate that they would have undetectable C IV absorption, but large O VI and H I columns should be present. We attribute our lack of detection of the O VI and Ly $\beta$  absorption from the X-ray absorbers to a combination of noise and dilution of the nuclear spectrum by hot stars in the large *FUSE* aperture.

*Subject headings:* galaxies: individual (NGC 4395) – galaxies: Seyfert – ultraviolet: galaxies

## 1. Introduction

A majority ( $\sim 60\%$ ) of Seyfert 1 galaxies show outflow of ionized gas from their nuclei, as revealed by intrinsic ultraviolet (UV) and X-ray absorption lines that are blueshifted with respect to the systemic velocities of the galaxies. The significance of the outflows is illustrated by the fact that the inferred mass-loss rates are comparable to the mass-accretion rates (Crenshaw, Kraemer, & George 2003a). Dynamical models of the outflowing absorbers make use of thermal winds, radiation pressure, and/or hydromagnetic flows from the central accretion disk, presumably responsible for most of the continuum radiation, or from the nearby broad-line region or torus. To constrain the dynamical models, and in particular to test the hypothesis that radiation pressure is the driving force, it is important to determine their rate of occurrence and variation in properties as functions of the luminosity of the central continuum source.

At luminosities higher than those of Seyferts, a significant fraction of quasars (25% to 55%) show intrinsic absorption in the UV (Ganguly et al. 2001; Laor & Brandt 2002; Vestergaard 2003) and X-rays (George et al. 2000). However, the case for intrinsic absorption in low-luminosity active galactic nuclei (AGN) has not been firmly established. Shields et al. (2002) find that LINERs often show absorption lines, but these can usually be attributed

to the interstellar medium (ISM) in their host galaxies, and there is little evidence in most cases for absorbers outflowing from their nuclei.

To date, NGC 4395 provides the best case for a low-luminosity AGN with intrinsic absorption that could possibly be attributed to the nucleus. NGC 4395 is an Sd III-IV dwarf galaxy that harbors one of the nearest ( $d \approx 4.6$  Mpc, Karachentsev et al. 2003) and least luminous ( $L_{bol} \approx 5 \times 10^{40}$  ergs s $^{-1}$ , Moran et al. 2004) AGN known. The active nucleus can be thought of as a dwarf Seyfert 1, since it possesses a bright central continuum source that is rapidly variable in the X-rays (Lira et al. 1999; Moran et al. 1999, 2004; Shih et al. 2003, hereafter SH2003) as well as broad and narrow emission lines that are photoionized by the central source (Kraemer et al. 1999). A variety of evidence indicates that the nucleus harbors a relatively low mass ( $10^4 - 10^5 M_{\odot}$ ) black hole that is responsible for powering the nuclear activity (Filippenko & Ho 2003). The broad permitted lines, strong high-ionization lines (Kraemer et al. 1999), and relatively high accretion rate ( $L_{bol}/L_{Edd} \approx 2 - 20 \times 10^{-3}$ ) compared to that of LINERs ( $L_{bol}/L_{Edd} < 10^{-3}$ , see Ho 1999) strongly support the Seyfert 1 interpretation for NGC 4395.

Several previous studies of NGC 4395 have made a case for intrinsic UV or X-ray absorption from ionized gas in the line of sight to the nucleus. Faint Object Spectrograph (FOS) observations obtained at low spectral resolving power ( $\lambda/\Delta\lambda \approx 1000$ ) with the *Hubble Space Telescope* (*HST*) show absorption features in the blue wing of the C IV emission line, at the observed wavelengths of 1544 and 1550 Å (Filippenko, Ho, & Sargent 1993; Kraemer et al. 1999). Early X-ray observations with *ROSAT* (Lira et al. 1999; Moran et al. 1999) and *ASCA* (Iwasawa et al. 2000) showed evidence for absorption in soft X-rays, indicative of one or more X-ray “warm absorbers.” Subsequent *Chandra X-ray Observatory* (*CXO*) (Moran et al. 2004) and long *ASCA* (SH2003) observations showed a downturn in the X-ray spectrum at  $E \lesssim 3$  keV, apparently due to absorption from highly ionized gas.

In an effort to confirm the presence of intrinsic UV absorption in NGC 4395, and determine its properties and connection with the claimed X-ray absorption, we have obtained new observations with the *Far Ultraviolet Spectroscopic Explorer* (*FUSE*) and the Space Telescope Imaging Spectrograph (STIS) on *HST*. We were also motivated by our previous study of the emission-line regions in NGC 4395 (Kraemer et al. 1999), which revealed that both the broad-line region (BLR) and narrow-line region (NLR) should have large ( $\gtrsim 50\%$ ) covering factors of the central source, and thus might be detectable in absorption.

## 2. Observations

We observed the nucleus of NGC 4395 contemporaneously with *FUSE* and STIS at high spectral resolutions, to identify possible absorption systems in the UV. We obtained the *FUSE* observations on 2003 February 25 UT with a total exposure time of 36,000 s. We used the standard  $30'' \times 30''$  low-resolution aperture (LWRS), which samples a much larger circumnuclear region than our STIS observation (see below). We processed the *FUSE* data with version 2.2.3 of the standard calibration pipeline, CALFUSE, which extracts spectra for each of the eight combinations of channels (SiC1, SiC2, LiF1, LiF2) and detector segments (A and B). Curvature in the LiF1B spectrum due to the anomalous feature known as “the worm” (Sanhow et al. 2002) was corrected by comparison to the LiF2A spectrum. The channel/segments with overlapping wavelength coverage with the LiF1a spectrum were scaled to match its flux. All spectra were then co-added by weighting each channel/segment by its effective area, using the effective area versus wavelength functions given in Blair et al. (2000). The final calibrated spectrum covers the range 905 – 1180 Å at a velocity resolution of  $\sim 15 \text{ km s}^{-1}$  (full-width at half-maximum [FWHM] of the line-spread function).

We obtained STIS echelle spectra of the nucleus of NGC 4395 through the  $0''.2 \times 0''.2$  aperture on 2003 March 9 UT. We used the E140M grating over three consecutive *HST* orbits to yield a total exposure time of 8022 s; the spectra cover the range 1150 – 1730 Å at a velocity resolution of  $\sim 7 \text{ km s}^{-1}$  (FWHM). We also obtained a 2182 sec exposure with the E230M grating during one orbit to cover the range 2271 – 3119 Å at a velocity resolution of  $\sim 10 \text{ km s}^{-1}$  (FWHM). We reduced the STIS spectra using the IDL software developed at NASA’s Goddard Space Flight Center for the STIS Instrument Definition Team. The data reduction included a procedure to remove the background light from each order using a scattered light model. The individual orders in each echelle spectrum were spliced together in the regions of overlap.

We measured the continuum fluxes of the three individual STIS E140M spectra and found no significant ( $\geq 10\%$ ) variations on short time scales (i.e., from one  $\sim 90$  min orbit to the next). The average and standard deviation of the continuum fluxes at 1345 Å (in a bin of 30 Å) are  $1.55 (\pm 0.11) \times 10^{-15} \text{ ergs s}^{-1} \text{ cm}^{-2} \text{ Å}^{-1}$ . This happens to be close to the 1345 Å continuum flux from the FOS spectrum obtained on 1992 July 15, 19 (Filippenko, Ho, & Sargent 1993):  $1.41 \times 10^{-15} \text{ ergs s}^{-1} \text{ cm}^{-2} \text{ Å}^{-1}$ . Given the lack of obvious variability on 90-minute time scales, we averaged the E140M spectra together to improve the signal-to-noise ratio.

### 3. Hot Stars in the FUSE Aperture

Comparison of the STIS and *FUSE* spectra in the region of overlap (1150 – 1180 Å) reveals that the *FUSE* continuum flux is 3.0 times higher than that from STIS. Although we cannot rule out variability in the UV continuum flux over the 12-day interval between the observations, we demonstrate that the principal source of the flux discrepancy is the presence of hot stars in the large *FUSE* aperture. This is not surprising, since there is intense star formation occurring throughout NGC 4395 (Cedr s & Cepa 2002).

Given that there are no available far-UV images of NGC 4395 (which will change with the release of the GALEX all-sky survey), we test the hot-star hypothesis in three ways: with a near-UV image, with the H $\alpha$  images of Cedr s & Cepa (2002), and by comparing the *FUSE* spectrum with starburst models from Leitherer et al. (1999). We have examined a near-UV image (centered at 3300Å) obtained with the Advance Camera for Surveys (ACS) on *HST* on 2002 October 27 UT. The integrated flux in the 25''  $\times$  28'' ACS image, which is close to the projected area of the *FUSE* aperture, is 3.1 times that measured in a region corresponding to the STIS aperture (H.R. Schmitt et al. 2003, in preparation), in close agreement with the far-UV ratio measured from the spectra.

Cedr s & Cepa (2002) detected three H $\alpha$  sources inside the region covered by the *FUSE* aperture: the nucleus, a source  $\sim 7''$  to the E, and another source  $\sim 5''$  to the S of the nucleus (regions 99, 98 and 97, respectively, in their paper). Assuming that all the nuclear H $\alpha$  emission is ionized by the AGN, we get that  $F(\text{H}\alpha) = 4.45 \times 10^{-14}$  ergs s $^{-1}$  cm $^{-2}$  for the other two sources. Based on this value, we calculate from equation (2) in Kennicutt (1998) that this corresponds to a star formation rate of  $8.4 \times 10^{-4}$  M $_{\odot}$  yr $^{-1}$ . This star formation rate corresponds to a far-ultraviolet flux of  $F_{\lambda}(1150 \text{ \AA}) = 5.7 \times 10^{-15}$  ergs s $^{-1}$  cm $^{-2}$  Å $^{-1}$  using equation (1) in Kennicutt (1998). These calculations are based on a continuous star formation rate over a period of  $\sim 100$  Myr, which can give different results from the ones obtained using an instantaneous burst. According to Cedr s & Cepa (2002), the equivalent widths of H $\alpha$  emission are  $\log(\text{EW}/\text{\AA}) = 2.46$  and 2.61 for regions 97 and 98, respectively. Using the Starburst99 models for an instantaneous burst with metallicity 0.4 solar and Salpeter IMF (Leitherer et al. 1999), we find that these equivalent widths correspond to bursts with ages of  $\sim 5$  Myr. Scaling the 5 Myr model to match the observed H $\alpha$  flux, we get a continuum flux of  $F_{\lambda}(1150 \text{ \AA}) = 8.5 \times 10^{-15}$  ergs s $^{-1}$  cm $^{-2}$  Å $^{-1}$ . Both of these estimates are close to the excess far-UV flux in the *FUSE* aperture of  $F_{\lambda}(1150 \text{ \AA}) = 5.9 (\pm 1.1) \times 10^{-15}$  ergs s $^{-1}$  cm $^{-2}$  Å $^{-1}$ .

The third test for the hot stars hypothesis was done by comparing the *FUSE* spectrum with starburst models created using Starburst99 (Leitherer et al. 1999), which incorporate far-UV stellar spectra from Robert et al. (2003). The models assume an instantaneous burst

with a Salpeter IMF, upper and lower mass limits of  $100 M_{\odot}$  and  $1 M_{\odot}$ , respectively, and a metallicity of  $0.4Z_{\odot}$ , which is consistent with the values measured by Cedrés & Cepa (2002). We restrict our comparison of the FUSE spectrum to models with ages between 3 Myr and 7 Myr, which is consistent with the age obtained for regions 97 and 98 based on the equivalent widths of  $H\alpha$ . In order to compare the FUSE spectrum with the starburst models, we first corrected the spectrum of NGC 4395 for Galactic reddening, using the value  $E(B-V) = 0.074$  from Schlegel, Finkbeiner & Davis (1998). Internal reddening is not a problem in the nucleus of this galaxy (Ho, Filippenko & Sargent 1997). We then corrected the spectrum for redshift, and resampled it to  $0.13 \text{ \AA}$  in wavelength, which is the spectral resolution of the models.

The resulting spectrum is presented as a thin line in Figure 1. Since approximately one third of the flux observed by FUSE at  $1150 \text{ \AA}$  originates at the nucleus, we used the *HST* spectrum to determine the slope of the AGN continuum and extrapolate it to lower wavelengths. We did this by fitting a power law ( $F_{\lambda} \propto \lambda^{\alpha}$ ) to the continuum regions in the wavelength range  $1268 - 1730 \text{ \AA}$  (thereby avoiding possible contamination from stars at longer wavelengths). We found that the AGN continuum can be represented by a power law with slope  $\alpha = -0.59 \pm 0.58$ . The extrapolation of this power law to shorter wavelengths is shown as a thick dotted line in Figure 1. We also show a spectrum from a 5 Myr starburst model (thick solid line), scaled so that when added to the power law, its flux is the same as the one observed in NGC 4395 over the wavelength range  $1102-1107 \text{ \AA}$ . Due to the low S/N ratio of the *FUSE* spectrum of NGC 4395, we did not attempt a detailed modeling of the stellar absorption lines; comparison with starburst spectra with ages between 3 Myr and 7 Myr did not show a significant difference, so we adopted the model which corresponded to the age determined from the  $H\alpha$  equivalent widths. Most of the absorption lines detected in the spectrum are due to interstellar gas in our Galaxy or NGC 4395. However, several stellar absorption lines, notably from C III, S IV, P V and Si IV, are clearly present (we could not detect O VI absorption because it is filled in with emission from the AGN). The strengths of these lines are similar in NGC 4395 and in the model spectrum. A subtraction of the starburst plus power law model from the spectrum of NGC 4395 (bottom panel of Figure 1) successfully removes the strongest stellar and large-scale continuum features, leaving residuals primarily due to interstellar absorption and nuclear emission lines. Based on all the tests presented in this section, we conclude that a starburst is the correct explanation for the excess emission observed by FUSE. This turns out to have important consequences for the detection of intrinsic absorption in the *FUSE* aperture (§5.3).

#### 4. Detection and Measurement of Intrinsic UV Absorption

Due to the relative faintness of NGC 4395, its STIS spectra are noisier than the STIS echelle spectra of other Seyfert galaxies that we have studied in the past (Crenshaw et al. 2003a). The signal-to-noise ratio per resolution element is  $S/N = 2.3$  in the regions of broad C IV emission surrounding the intrinsic absorption, whereas  $S/N \approx 8$  in these regions for similar exposure times in NGC 5548 (Crenshaw et al. 2003b). For the *FUSE* spectra, we estimate  $S/N \approx 3$  (per resolution element) in the O VI region. Since intrinsic absorption lines are expected to encompass many resolution elements (Crenshaw et al. 1999), we smoothed the spectra by a 7-point boxcar function to search for absorption lines.

Figure 2 shows portions of the STIS echelle spectra in regions where we have detected absorption lines that are likely to be intrinsic to NGC 4395. From the narrow emission lines of the C IV doublet seen in the top panel, we have determined an emission-line redshift of  $z = 0.0012$ , close to the value of 0.0011 determined from H I 21-cm emission by Haynes et al. (1998). We note that these emission lines are unusually narrow compared to those of normal Seyfert galaxies; for C IV the FWHM is  $65 \text{ km s}^{-1}$ , similar to the value of  $\sim 50 \text{ km s}^{-1}$  determined for various narrow emission lines from a high-resolution optical spectrum of NGC 4395 (Filippenko & Ho 2003). Unfortunately, the N V  $\lambda\lambda 1238.8, 1242.8$  region is very noisy, and no absorption (not even Galactic) was detected in this region. Strong, broad Galactic Ly $\alpha$  absorption prevents detection of any intrinsic Ly $\alpha$  absorption.

Most of the absorption lines that we have detected in the STIS spectra can be attributed to the Galaxy, at a radial velocity of  $-29 \text{ km s}^{-1}$  in the observed frame ( $-389 \text{ km s}^{-1}$  in Figure 2). However, we have identified two possible kinematic components of absorption that could be intrinsic to NGC 4395. Component 1 at  $-770 \text{ km s}^{-1}$  (with respect to  $z = 0.0012$ ) is only evident in the C IV  $\lambda 1548.2$  line. The associated C IV  $\lambda 1550.8$  line is blended with Galactic absorption, so we regard this identification as tentative. There is little or no low-ionization gas associated with this component; in particular, there is no obvious Mg II absorption. Component 2 at  $-114 \text{ km s}^{-1}$  is seen in the lines of C IV  $\lambda\lambda 1548.2, 1550.8$ , Si IV  $\lambda\lambda 1393.8, 1402.8$ , Mg II  $\lambda\lambda 2796.3, 2803.5$ , and O I  $\lambda 1302.2$  (also C II  $\lambda 1334.5$ , which is not shown). Although the lines from Component 2 do not align perfectly, it is not possible to determine if this is due to ion-dependent velocity structure or just noise. Component 2 appears to be heavily saturated in all lines except for C IV. In the top panel of Figure 2, we have overplotted the 1992 FOS spectrum (corrected to match the STIS spectrum by adding  $2 \text{ \AA}$  to the wavelength scale). The two broad dips in the FOS spectrum correspond to our claims of absorption features at 1544 and 1550  $\text{\AA}$  (Filippenko, Ho, & Sargent 1993; Kraemer et al. 1999). These can now be attributed to blends of the intrinsic and Galactic absorption lines that we have identified in the STIS spectrum, plus some contribution of the

gap between the narrow C IV emission doublet to the dip at 1550 Å (+ 300 km s<sup>-1</sup> in the plot).

Figure 3 shows portions of the *FUSE* spectra. Due to the low S/N at short wavelengths, we were unable to detect even Galactic absorption in the expected lines of C III  $\lambda$ 977.0 and N III  $\lambda$ 989.8. However, Ly $\beta$  and C II  $\lambda$ 1036.3 are clearly present in Component 2. The Ly $\beta$  absorption at Component 2 is not just the wing of the Galactic component, since symmetric absorption is not present on the other (more negative) side of geocoronal Ly $\beta$  emission. As the top panel of Figure 3 shows, we have not detected O VI absorption in any component, despite the reasonably decent S/N (the absorption near the expected locations of Components 1 and G in O VI  $\lambda$ 1037.6 is due to C II, as shown in the bottom panel).

To further characterize the absorption components, we have measured their radial velocity centroids and equivalent widths (EWs) assuming full coverage of the continuum and line emission. We determined uncertainties in the absorption measurements from photon statistics and different reasonable placements of the continuum and emission-line profiles. Since these data are too noisy to determine covering factors and ionic column densities from the optical depths of the lines, we have estimated column densities for Components 1 and 2 from the EWs of the lines. As mentioned previously, nearly all of the detected lines appear to be saturated, so we used the EWs to calculate lower limits to their columns. Since C IV does not appear to be saturated in Component 2, we give an actual value and estimated error for its column. Note that if the covering factor for C IV is significantly less than one, which seems unlikely given the depths of the other lines in this component, the quoted value for the C IV column density is a lower limit.

Our measurements are summarized in Table 1. In addition to the velocity centroids and EWs for Component 2, we list the corresponding Galactic values for comparison. For the Galactic component, the average velocity centroid is  $-29 (\pm 20)$  km s<sup>-1</sup> in the observed frame. For Component 2, the average velocity centroid is  $-114 (\pm 21)$  km s<sup>-1</sup> with respect  $z = 0.0012$ , and the FWHM of the unsaturated C IV absorption is  $60 (\pm 22)$  km s<sup>-1</sup>. If Component 1 is real and outflowing with respect to  $z = 0.0012$ , we estimate a radial velocity and FWHM of  $-770 (\pm 21)$  and  $130 (\pm 30)$  km s<sup>-1</sup>, respectively. An EW of  $0.84 (\pm 0.21)$  Å gives a lower limit of  $2.0 (\pm 0.5) \times 10^{14}$  cm<sup>-2</sup> for the C IV column density in Component 1.

## 5. Origin of the Absorption

In general, the absorption components that we have detected could arise in 1) our Galaxy (disk or halo), 2) the ISM of NGC 4395, 3) the NLR of NGC 4395, 4) outflowing UV absorbers

similar to those found in most Seyfert 1 galaxies, or 5) X-ray absorbers, characterized by higher ionization parameters than those of typical UV absorbers (Crenshaw et al. 2003a). We detect a number of absorption lines from the Galaxy (Component “G”) at an observed radial velocity of  $-29 \text{ km s}^{-1}$ ; their EWs are similar to those found in other studies of Galactic absorption (Savage & Sembach 1994). Since the redshift of NGC 4395 is low, and absorption lines from the Galactic halo can appear at radial velocities of several hundreds of  $\text{km s}^{-1}$  in the observed frame, we need to consider the possibility of a Galactic origin for the other absorption components. We rule out a Galactic origin for Component 2, at a radial velocity of  $+246 \text{ km s}^{-1}$  in the observed frame, since at the Galactic coordinates for NGC 4395 ( $l = 162.2^\circ$ ,  $b = 81.5^\circ$ ), all of the high-velocity HI (Wakker 1991) and O VI (Sembach et al. 2003) clouds detected in this area of the sky have negative radial velocities (Wakker 1991). Component 1 is at a radial velocity  $-410 \text{ km s}^{-1}$  in the observed frame; although it could conceivably originate in the Galactic halo, its velocity is at least  $100 \text{ km s}^{-1}$  more negative than other H I and O VI halo clouds in this area of the sky (Wakker 1991; Sembach et al. 2003). Also, we would expect to see detectable Si IV for this component if it were halo gas (Savage & Sembach 1994), and none is apparent (see Figure 2). Thus, it is likely that these two components do not arise from the Galaxy.

Given an intrinsic origin for Components 1 and 2, the distinction between the above sources may seem somewhat ambiguous. For example, some outflowing UV absorbers are likely a component of the NLR (Kraemer et al. 2001), while others have been linked to X-ray absorbers, such that the UV absorption lines are due to trace elements in the highly ionized, high-column gas (Mathur et al. 1994; Kraemer et al. 2002). For this discussion, the intrinsic absorption components are placed into the general category of outflowing UV absorber if they are not consistent with an origin in the other categories, which have been well characterized in NGC 4395 by other studies, as discussed in the following subsections.

### 5.1. Component 1

First, we need to consider whether or not Component 1 is “real,” given the detection of one C IV absorption line in noisy data. On the positive side, there is an inflection in the FOS spectrum at this position that appears to be distinct from the inflection caused by the Galactic C IV  $\lambda 1548.2$  line (Figure 2). On the negative side, no other lines have been detected, and in particular, Ly $\beta$  appears to be absent at the radial velocity of Component 1. We have been unable to devise a photoionization model that would result in an undetectable Ly $\beta$  line, since even very highly ionized gas will have a substantial H I column. Assuming the C IV absorption is real, the associated Ly $\beta$  absorption must be diluted by unabsorbed

UV continuum emission in the *FUSE* aperture, which we characterized in §3.

The high radial velocity of Component 1 ( $-770 \text{ km s}^{-1}$ ) with respect to NGC 4395 rules out an origin in the ISM of this galaxy. As can be seen in Figures 2 and 3, the wings of the narrow components of the emission lines do not extend past about  $\pm 100 \text{ km s}^{-1}$  from line center, so an origin in the NLR is ruled out as well. As discussed in §5.3, the X-ray absorbers characterized by SH2003 are too highly ionized to produce significant columns of C IV or lower-ionization species. Thus, Component 1 likely originates in an outflowing UV absorber, which is defined by the presence of C IV absorption that is blueshifted with respect to the systemic velocity of the host galaxy (Crenshaw et al. 1999). The absence of Si IV and lower ionization lines is not a problem for this interpretation, since most UV absorbers are too highly ionized to have substantial columns of these ions (Crenshaw et al. 1999, 2003a). In this case, one would expect detectable (and likely saturated) columns of O VI and H I, which are not seen at the position of Component 1 (see Figure 3). The expected O VI and Ly $\beta$  absorption lines are likely “hidden” by a substantial contribution from unabsorbed UV continuum emission, as demonstrated in §5.3.

## 5.2. Component 2

It is instructive to compare our measurements of Component 2 with those of the Galactic component in Table 1. Since Component 2 is close to the systemic velocity (although with a slight blueshift), it could arise from the ISM of the host galaxy. However, an origin in the NLR or X-ray absorbers cannot be ruled out by the kinematics alone, since the radial velocity of Component 2 ( $-114 \text{ km s}^{-1}$ ) is consistent with the small widths of the narrow emission lines, and we have no constraints on the kinematics of the X-ray absorbers.

We can obtain further insight by comparing the EWs of the lines from Component 2 with those of the Galaxy. In Table 1, the EWs of the low-ionization lines are very similar, whereas those of the higher ionization lines of Si IV and C IV are about half the values of their Galactic counterparts. Component 2 could therefore arise from the ISM of NGC 4395, assuming it has a smaller amount of high-ionization gas than the Galactic column along this particular line of sight. Moreover, we can rule out an origin in photoionized gas, regardless of whether it is the NLR, UV absorbers, or X-ray absorbers. The key is the ratio of  $N(\text{Si IV})/N(\text{C IV})$  which is  $\geq 1.5$ . Given a power-law continuum and the abundances in §5.3, we are unable to reproduce this ratio with photoionization models covering a broad range in ionization parameter and hydrogen column density. Our models predict this ratio should always be  $\leq 0.3$ , primarily due to the abundance ratio. However,  $N(\text{Si IV})/N(\text{C IV})$  ratios as high as  $\sim 1$  can be found in Galactic halo gas (Savage & Sembach 1994), which is

primarily collisionally ionized.

A final point in favor of an ISM origin is that the C II and Ly $\beta$  lines for Component 2 in the FUSE spectrum are saturated near the zero flux level. If these lines originated solely in either the NLR (with an angular size  $<0''.4$ , Filippenko et al. 1993) or absorbers near the nucleus, the extra far-UV flux in the large *FUSE* aperture would make them appear much shallower.

### 5.3. Connection to the X-ray Absorbers

We have generated photoionization models to further explore the possibility that the X-ray absorbers in NGC 4395 produce observable UV absorption lines. A long (640 ks) *ASCA* observation from 2000 revealed an underlying continuum characterized by a photon index  $\Gamma \approx 1.46$ , modified by a large column of gas intrinsic to NGC 4395, which SH2003 modeled as a two-zoned X-ray absorber. The zone closer to the nucleus was highly variable while the ionization state and total column density of the outer zone remained relatively constant during their observation. Both of the components are highly ionized, and their observed effect is a depression of the continuum below  $\sim 3$  keV, due to the combined effects of the bound-free edges of species such as O VII, O VIII, Ne IX, and Ne X. Notably, in their 17 ks *Chandra* spectrum, Moran et al. (2004) also found evidence for complex absorption, although these data are of insufficient quality to tightly constrain the physical characteristics of the absorber.

The large column densities predicted by SH2003 suggest that detectable columns of H I and O VI may arise within the X-ray absorber. To calculate these column densities, we used the photoionization code CLOUDY90 (Ferland et al. 1998) to regenerate the constant component from SH2003, which has a lower ionization than the variable component, and thus includes a larger fraction of the lower ionization species. For their models, SH2003 assumed that the X-ray continuum, with a spectral index  $\alpha = 0.46$ , extends to lower energies without turning up to meet the UV, which severely underpredicts the UV continuum. Therefore, we assumed a model spectral energy distribution (SED) closer to that which we derived for our emission-line study (Kraemer et al. 1999), with the form  $F \propto \nu^{-\alpha}$ , where  $\alpha = 1.7$  for  $13.6 \leq h\nu < 1000$  eV, and  $\alpha = 0.46$  for  $h\nu \geq 1000$  eV. SH2003 use the ionization parameter  $\xi$  (in  $\text{erg cm s}^{-1}$ ), which is  $395.3 \times U$  for their adopted SED, where  $U$  is the number of ionizing photons per H atom. Based on our SED, we fixed the flux at 0.5 keV in order to predict the same H-like and He-like O and Ne columns, and hence the same opacity near 1 keV. This results in a factor of 28.5 increase in  $U$ , due to the larger number of EUV photons. So for the constant component of the X-ray absorber modeled by SH2003, their value  $\xi = 200$

corresponds to  $U = 14.4$ .

Assuming solar abundances, SH2003 derive a total hydrogen column density  $N_H = 2.45 \times 10^{22} \text{ cm}^{-2}$ , for the constant component of the absorber. However, in our emission-line study (Kraemer et al. 1999), we determined that the heavy element abundances in the NLR of NGC 4395 were sub-solar, with most elements  $\sim 1/2$  solar by number with respect to H, and  $N/H \approx 1/6$  solar. Therefore, in order to reproduce the X-ray opacity from the SH2003 model, we increased the total column density to  $N_H = 4.0 \times 10^{22} \text{ cm}^{-2}$ . We assumed that the X-ray absorber is free of cosmic dust and all elements are in the gas phase.

In Table 2, we compare our predictions of ionic column densities from models using the SH2003 SED and our revised SED. The high-ionization columns derived from the X-ray observations are essentially the same. However, the H I and O VI column densities are factors of  $\sim 17$  and  $\sim 4$  smaller, respectively, in the model that uses our more realistic SED, due to the much larger flux of UV photons. Nevertheless, these columns are still quite large, and should be detectable in the *FUSE* band if the entire source of UV continuum emission is covered. Our revised SED model predicts undetectable columns of C IV ( $3.4 \times 10^{11} \text{ cm}^{-2}$ ) and other low-ionization lines, so these lines in Components 1 and 2 are not from the X-ray absorbers.

So where are the expected H I and O VI absorption lines from the X-ray absorbers of SH2003? Given their column densities from our revised SED model in Table 2, we have generated simulated absorption-line profiles to determine if they would be detectable in the *FUSE* spectra. For the purpose of illustration, we assumed that the X-ray component has the radial velocity and FWHM ( $= 60 \text{ km s}^{-1}$ ) of Component 2. In Figure 3, we overplot the simulated absorption lines for two cases: complete covering of the UV continuum and 50% covering in the line of sight. The latter comes from assuming that the broad-line emission is covered and that the excess continuum flux in the *FUSE* is not, resulting in a continuum covering factor of 0.33 and an effective covering factor of  $\sim 0.5$  at the Component 2 positions. Figure 3 demonstrates that for complete covering, the Ly $\beta$  absorption from the X-ray absorber would be detectable, unless it is hidden in the low-ionization gas associated with Component 2 or filled in by geocoronal Ly $\beta$  emission. O VI absorption at full covering would be detectable at Component 2 or any other velocity, unless it is fortuitously covered by the narrow O VI emission at the systemic velocity of NGC 4395, in which case it would not be outflowing. For the case of 50% covering, the H I and O VI absorption could be present at Component 2 or any other radial velocity, given the noise level of the *FUSE* spectra. Thus, although we do not detect the expected O VI and H I absorption lines, the *FUSE* spectra are not inconsistent with the parameters derived for the X-ray absorbers by SH2003.

## 6. Conclusions

We confirm the detection of C IV absorption in NGC 4395, and have identified a number of other absorption lines in new high-resolution *FUSE* and *HST/STIS* spectra. In addition to Galactic lines, we have identified two components that are likely to be intrinsic to NGC 4395. Component 1 at  $-770 \text{ km s}^{-1}$  (with respect to  $z = 0.0012$ ) is only detected in the C IV  $\lambda 1548.2$  line. If it is real, it cannot arise in the ISM or NLR of NGC 4395 due to its high velocity. Furthermore, the X-ray absorbers characterized by SH2003 are too highly ionized to produce a detectable C IV column. Thus, Component 1 likely originates in an outflowing UV absorber similar to those seen in most Seyfert 1 galaxies (Crenshaw et al. 2003a). Observations at higher S/N are required to confirm the reality of this component, and identify additional lines (e.g., N V  $\lambda\lambda 1238.8, 1242.8$ ) to characterize its physical conditions.

The possibility that Component 1 arises from UV absorbers close to the nucleus, for example in an accretion-disk wind (e.g., Proga 2003), remains an intriguing prospect, given the low luminosity of the central continuum source. Drawing on the analogy with UV absorbers in normal Seyfert 1s, possible indicators of a location close to the nucleus would be variability in the absorption lines or partial covering of the continuum and/or BLR. These measurements require high-resolution spectra at higher S/N than the current data.

Component 2 shows a broad range in ionization, and likely arises in the ISM of NGC 4395, since photoionization models cannot match the observed  $N(\text{Si IV})/N(\text{C IV})$  ratio, and the C II and  $\text{Ly}\beta$  absorption lines absorb all of the far-UV flux in the large ( $30'' \times 30''$ ) *FUSE* aperture. It is interesting that this component shows a slight outflow ( $-114 \text{ km s}^{-1}$ ) with respect to the host galaxy. This may indicate a large-scale galactic outflow driven by stellar winds and/or supernovae (Veilleux et al. 2002) near the center of the galaxy.

We have not detected the NLR in absorption, despite its large derived covering factor (Kraemer et al. 1999). This could be due to the overall geometry of the NLR or to clumpiness on a smaller scale (i.e., there is no NLR “cloud” in the line of sight to the continuum source). However, we note that absorption from the “OUTER” component of the NLR in Kraemer et al. could be hidden in Component 2 (the other NLR components have saturated C IV columns) if it shares the same outflow velocity as the ISM. We also do not detect the expected columns of O VI and  $\text{Ly}\beta$  absorption from the X-ray absorbers claimed by SH2003. This is likely due to a large contribution of hot stars to the far-UV flux in the *FUSE* aperture, although X-ray observations at higher S/N and spectral resolution would be helpful for confirming the presence and properties of the X-ray absorption.

We thank D. Shih, K. Iwasawa, and E. Moran for helpful discussions. SBK and DMC

acknowledge support from NASA grants HST GO-09362.01 and NAG5-13049. Support for proposal GO-9362 was provided by NASA through a grant from the Space Telescope Science Institute, which is operated by the Association of Universities for Research in Astronomy, Inc., under NASA contract NAS 5-26555. The National Radio Astronomy Observatory is a facility of the National Science Foundation, operated under cooperative agreement by Associated Universities, Inc.

## REFERENCES

- Blair, W. 2000, The *FUSE* Observers Guide, Version 2.1
- Cedr s, B. & Cepa, J. 2002, *A&A*, 391, 809
- Crenshaw, D.M., Kraemer, S.B., Boggess, A., Maran, S.P., Mushotzky, R.F., & Wu, C.-C. 1999, *ApJ*, 516, 750
- Crenshaw, D.M., Kraemer, S.B., & George, I.M. 2003a, *ARA&A*, 41, 117
- Crenshaw, D.M., et al. 2003b, *ApJ*, 594, 116
- Ferland, G.J., Korista, K.T., Verner, D.A., Ferguson, J.W., Kingdon, J.B., & Verner, E.M. 1998, *PASP*, 110, 761
- Filippenko, A.V., & Ho, L.C. 2003, *ApJ*, 588, L13
- Filippenko, A.V., Ho, L.C., & Sargent, W.L.W. 1993, *ApJ*, 410, L75
- Filippenko, A.V., & Sargent, W.L.W. 1989, *ApJ*, 342, L11
- Ganguly, R., Bond, N.A., Charlton, J.C., Eracleous, M., Brandt, W.N., & Churchill, C.W. 2001, *ApJ*, 549, 133
- George, I.M., et al. 2000, *ApJ*, 531, 52
- Haynes, M.P., van Zee, L., Hogg, D.E., Roberts, M.S., & Maddalena, R.J. 1998, *AJ*, 115, 62
- Ho, L.C. 1999, *ApJ*, 516, 672
- Ho, L.C., Filippenko, A.V. & Sargent, W.L.W. 1997, *ApJS*, 112, 315
- Iwasawa, K., Fabian, A.C., Almaini, O., Lira, P., Lawrence, A., Hayashida, K., & Inoue, H. 2000, *MNRAS*, 318, 879
- Karachentsev, I.D., et al. 2003, *A&A*, 398, 467
- Kennicutt, R.C. 1998, *ARA&A*, 36, 189
- Kraemer, S.B., Crenshaw, D.M., George, I.M., Netzer, H., Turner, T.J., & Gabel, J.R. 2002, *ApJ*, 577, 98
- Kraemer, S.B., Ho, L.C., Crenshaw, D.M., Filippenko, A.V., & Shields, J.C. 1999, *ApJ*, 520, 564
- Kraemer, S.B., et al. 2001, *ApJ*, 551, 671
- Laor, A., & Brandt, W.N. 2002, *ApJ*, 569, 641
- Leitherer, C., et al. 1999, *ApJS*, 123, 3
- Lira, P., Lawrence, A., O’Brien, P., Johnson, A., Terlevich, R., & Bannister, N. 1999, *MNRAS*, 305, 109

- Mathur, S., Wilkes, B., Elvis, M., & Fiore, F. 1994, *ApJ*, 434, 493
- Moran, E.C., Eracleous, M., Leighly, K.M., Chartas, G., Filippenko, A.V., Ho, L.C., & Blanco, P.R., 2004, submitted to *AJ*
- Moran, E.C., Filippenko, A.V., Ho, L.C., Shields, J.C., Belloni, T., Comastri, A., Snowden, S.L., & Sramek, R.A. 1999, *PASP*, 111, 801
- Pellerin, A. et al. 2002, *ApJS*, 143, 159
- Proga, D. 2003, *ApJ*, 585, 406
- Robert, C., Pellerin, A., Aloisi, A., Leitherer, C., Hoopes, C. & Heckman, T.M. 2003, *ApJS*, 144, 21
- Sahnow, D. 2002, *The FUSE Instrument and Data Handbook*, Version 2.1
- Savage, B.D., & Sembach, K.R. 1994, *ApJ*, 434, 145
- Schlegel, D.J., Finkbeiner, D.P. & Davis, M. 1998, *ApJ*, 500, 525
- Sembach, K.R., et al. 2003, *ApJS*, 146, 165
- Shields, J.C., Sabra, B.M., Ho, L.C., Barth, A.J., & Filippenko, A.V. 2002, in *Mass Outflow in Active Galactic Nuclei: New Perspectives*, ed. D.M. Crenshaw, S.B. Kraemer, & I.M. George (San Francisco: Astronomical Society of the Pacific), ASP Conference Series 255, 105
- Shih, D.C., Iwasawa, K., & Fabian, A.C. 2003, *MNRAS*, 341, 973 (SH2003)
- Veilleux, S., Cecil, G., Bland-Hawthorn, J., & Shopbell, P.L. 2002, *RevMexAA*, 13, 222
- Vestergaard, M. 2003, *ApJ*, 599, 116
- Wakker, B.P. 1991, in *IAU Symp. 144: The Interstellar Disk-Halo Connection in Galaxies*, ed. H. Bloemen (Dordrecht: Kluwer), p. 27

Fig. 1.— Reddening and redshift corrected *FUSE* spectrum of NGC 4395 (top panel) smoothed with a 5 point boxcar (thin line), the extension of the nuclear continuum to shorter wavelengths determined from the HST spectrum (thick dotted line), and the starburst model for an instantaneous burst 5 Myr old with metallicity  $0.4 Z_{\odot}$  and Salpeter IMF (thick solid line). The starburst spectrum is scaled so that, when added to the power law spectrum, the flux corresponds to that of NGC 4395 in the 1102 – 1107 Å range. This figure shows only the wavelength region covered by the models. The vertical dotted lines indicate interstellar absorption lines, from our Galaxy, obtained from the list of Pellerin et al. (2002). The most prominent stellar lines from the list of Pellerin et al. (2002) are indicated under the spectrum with thick bars. A number of H<sub>2</sub> absorption lines, not shown here, also contribute to absorption lines seen in this spectrum. The bottom panel of the figure shows the residuals from the subtraction of the starburst and power law spectrum from the spectrum of NGC 4395.

Fig. 2.— Portions of the STIS echelle spectra of NGC 4395, showing the absorption lines in different ions. The fluxes have been smoothed with a seven-point boxcar, and are plotted as a function of the radial velocity (of the strongest member for each doublet), relative to an emission-line redshift of  $z = 0.0012$ . The kinematic components of the lines (including doublets) are numbered, and strong Galactic absorption lines are labeled with “G”. The narrow components of the C IV emission are labeled with “n”. The 1992 *HST*/FOS spectrum is overplotted in the top panel in red.

Fig. 3.— Portions of the *FUSE* spectra of NGC 4395, plotted as in Figure 1. The absorption features in the region of O VI  $\lambda 1037.6$  are actually due to C II  $\lambda 1036.3$ , as shown in the bottom panel. The narrow components of O VI emission and geocoronal Ly $\beta$  emission are labeled with “n”. The simulated profiles described in §5.3 are plotted for 50% (blue) and 100% (red) covering of the continuum plus line emission.

Table 1. Measurements of Absorption Components in NGC 4395

Line	EW(G) <sup>a</sup> (Å)	$v_r$ (G) <sup>b</sup> (km s <sup>-1</sup> )	EW(2) <sup>a</sup> (Å)	$v_r$ (2) <sup>b</sup> (km s <sup>-1</sup> )	$N_{ion}(2)$ <sup>c</sup> (10 <sup>14</sup> cm <sup>-2</sup> )
Ly $\beta$ $\lambda$ 1025.7	—	—	0.86 ( $\pm$ 0.12)	–85	> 11.7
C II $\lambda$ 1036.3	0.48 ( $\pm$ 0.06)	–37	0.61 ( $\pm$ 0.10)	–104	>5.13
O I $\lambda$ 1302.2	0.52 ( $\pm$ 0.11)	–34	0.42 ( $\pm$ 0.12)	–124	>5.76
C II $\lambda$ 1334.5	0.91 ( $\pm$ 0.12)	–43	0.89 ( $\pm$ 0.10)	–115	—
Si IV $\lambda$ 1393.8	1.18 ( $\pm$ 0.19)	–18	0.43 ( $\pm$ 0.11)	–96	—
Si IV $\lambda$ 1402.8	—	—	0.55 ( $\pm$ 0.18)	–94	> 1.21
C IV $\lambda$ 1548.2	0.52 ( $\pm$ 0.07)	–16	0.25 ( $\pm$ 0.09)	–135	0.82 ( $\pm$ 0.29)
C IV $\lambda$ 1550.8	—	—	0.21 ( $\pm$ 0.09)	–155	—
Mg II $\lambda$ 2796.3	1.32 ( $\pm$ 0.27)	–33	1.63 ( $\pm$ 0.19)	–113	—
Mg II $\lambda$ 2803.5	0.92 ( $\pm$ 0.19)	–23	1.49 ( $\pm$ 0.24)	–118	>0.73

<sup>a</sup>Equivalent widths for kinematic Components “G” (Galactic) and “2”. See §4 for Component 1 C IV values.

<sup>b</sup>Radial velocity centroid relative to  $z = 0$  for Component G and  $z = 0.0012$  for Component 2. The uncertainty in these measurements is about  $\pm 10$  km s<sup>-1</sup>.

<sup>c</sup>Column density from the line that gives the tightest constraint for each ion.

Table 2. Warm Absorber Columns<sup>a</sup>

Ion	SH2003 SED (cm <sup>-2</sup> )	Revised SED (cm <sup>-2</sup> )
H I	$2.6 \times 10^{16}$	$1.5 \times 10^{15}$
O VI	$3.9 \times 10^{15}$	$1.1 \times 10^{15}$
O VII	$5.0 \times 10^{17}$	$5.3 \times 10^{17}$
O VIII	$4.9 \times 10^{18}$	$4.6 \times 10^{18}$
Ne IX	$5.1 \times 10^{17}$	$5.7 \times 10^{17}$
Ne X	$1.3 \times 10^{18}$	$1.2 \times 10^{18}$

<sup>a</sup>Predicted ionic column densities for the constant warm absorber of SH2003.

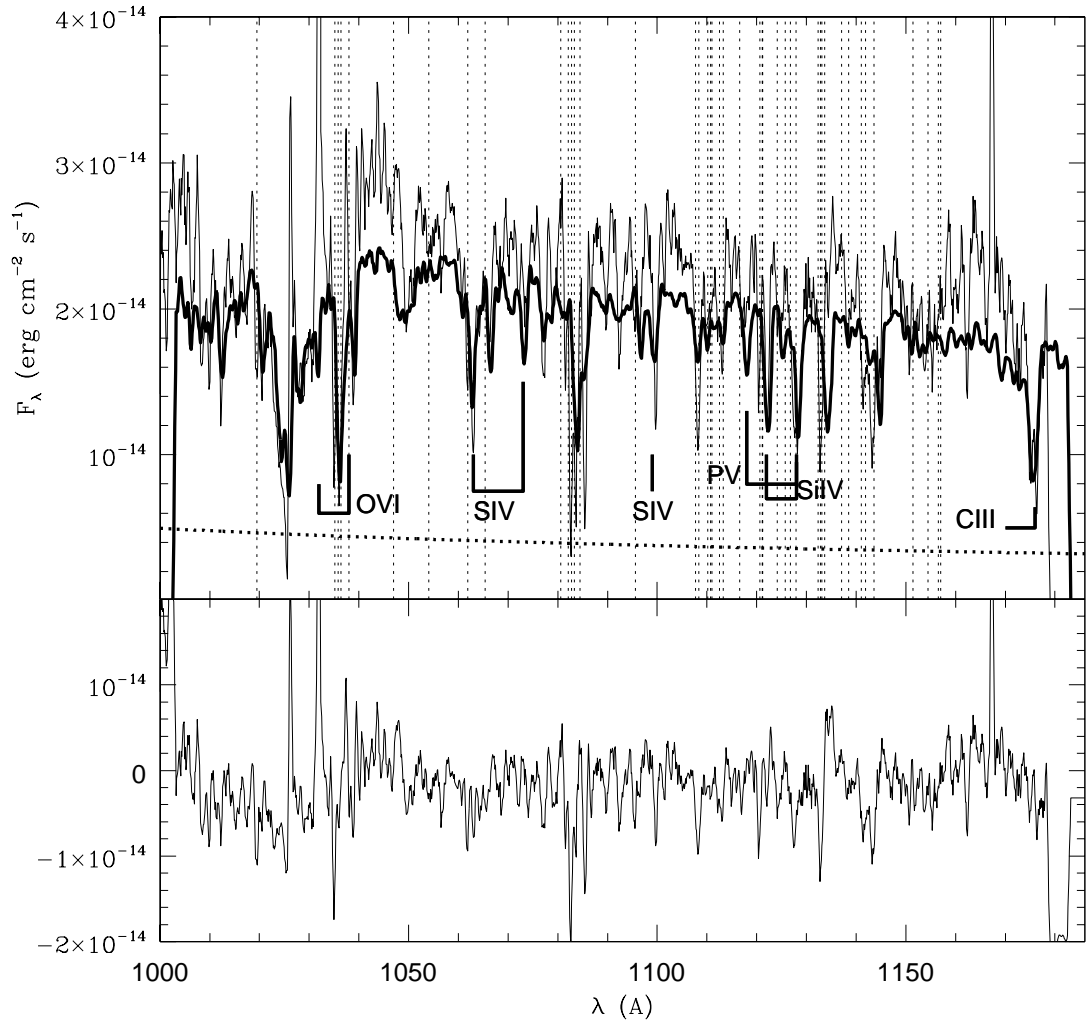


Fig. 1.

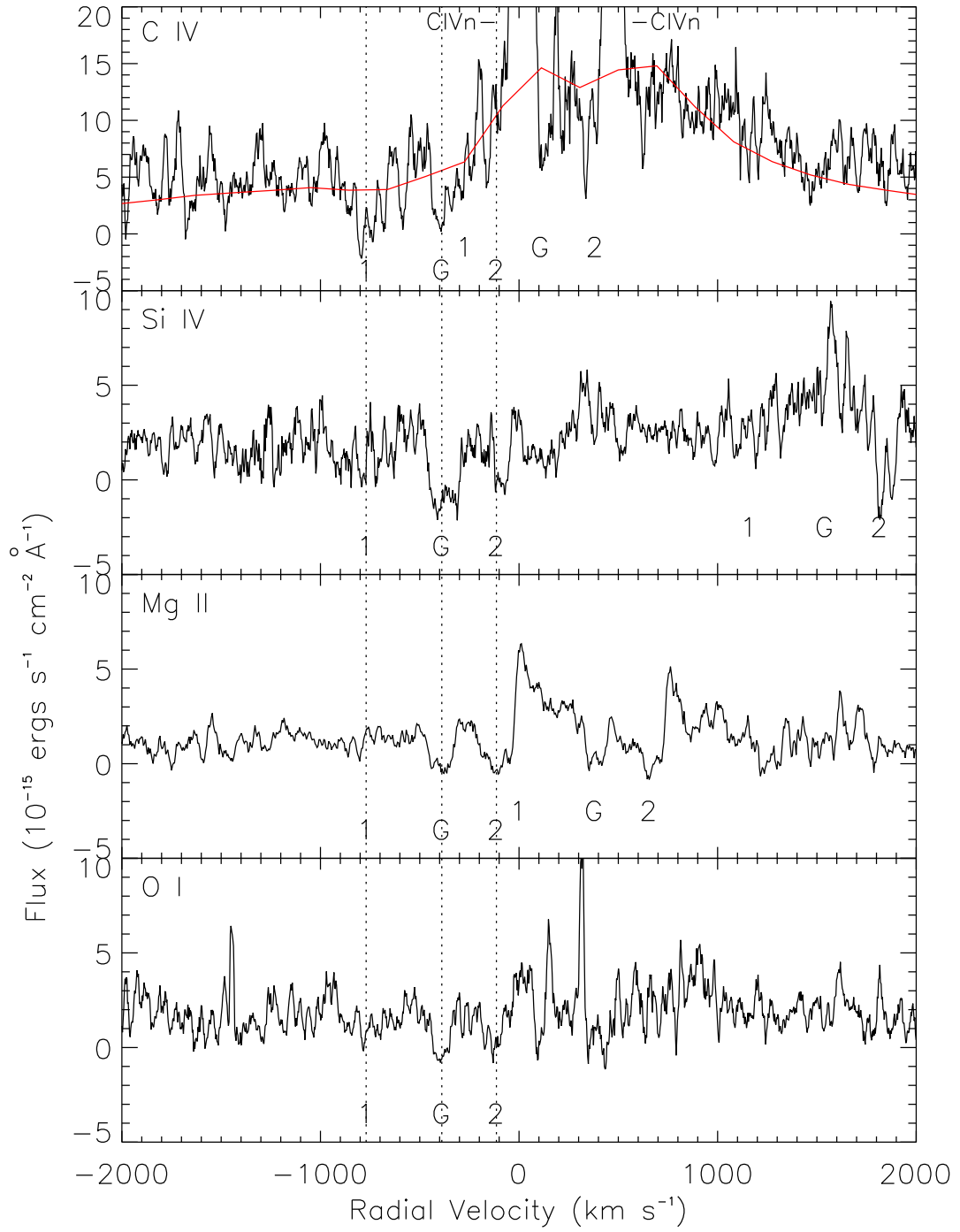


Fig. 2.

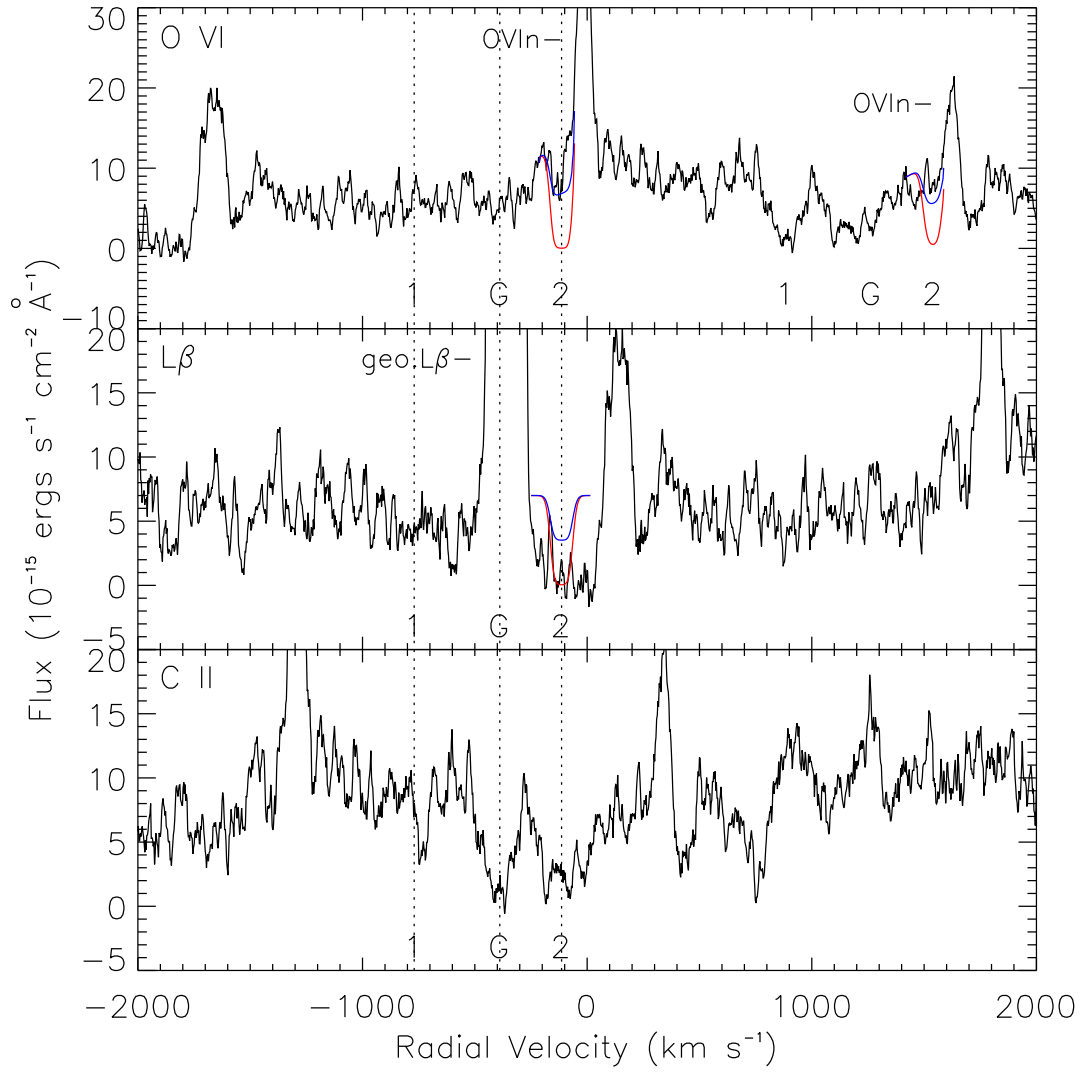


Fig. 3.